MARCO PIUMETTI[1]*, NIK LYGEROS[2]
*Corresponding author
1. Department of Applied Science and Technology, Politecnico di Torino, Corso Duca degli Abruzzi 24, 10129 Turin, Italy
2. Université de Lyon, LGPC (UMR 5285), 69616, Villeurbanne, France

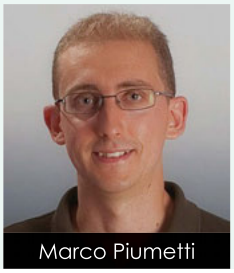
Marco Piumetti

From cooperative phenomena to synergetic hyperstructures in catalysis

KEYWORDS: Active sites, cooperation, game theory, hv-groups, hypergroups, hyperstructures theory, nash equilibrium, synergy.

Abstract Synergistic and cooperative phenomena in catalysis are defined here via a formal classification of the catalytic systems, using the combination of game theory and hyperstructure theory. Game theory is based on the idea that players are rational decision-makers; therefore, making a transposition is reported as rational, the chemical choice.
Three catalytic reactions are considered as characteristic examples: i) the degradation of an azo-dye (Acid Orange 7) with vanadium/hydrogen peroxide/ascorbic acid solutions (homogeneous catalysis); ii) the total oxidation of ethene and iii) the carbon monoxide oxidation over Cu-Ce mixed oxide catalysts (heterogeneous catalysis). According to the game theory, these reactions are paradigms of not-zero sum, asymmetrical and synchronous cooperative-games. The players (i.e. active phases/centres) exhibit a finite number of pure strategies, reflected by their concentrations, and play a strategic game. Moreover, there is the Nash equilibrium and even Pareto equilibrium in the synergistic case. Since the effects of the structural relations among players depend on the catalytic system, a scale of magnitude (in terms of catalytic benefits) is proposed: cooperation < synergetic hyperstructure << strong synergetic hyperstructure.

INTRODUCTION

In catalysis there are several characteristic examples in which the presence of two, or more, components may influence the catalytic activity of a catalyst by changing its solid-state chemistry (1). Many solid catalysts are multicomponent materials (e.g. bismuth molybdates, perovskites, heteropolyanions, vanadium phosphate, and so on) with active phases and promoters mutually-interacting each other over different domains (2-3). Thus, either cooperative or synergistic phenomena may appear and the catalytic behavior typically results in a non-linear combination of complexity structures of active sites (4-6). For instance, it has been shown through X-ray photoelectron spectroscopy (XPS) and electrical conductivity measurements that multicomponent catalysts, such as bismuth molybdates over Co(Fe)-molybdates, reveal synergistic effects due to the enhanced electrical conductivity of the Co(Fe)-molybdate support, attributable to the presence of both Fe^{2+} and Fe^{3+} in Co^{2+} molybdates, thus favouring the so-called Mars and van Krevelen (MvK) mechanism (7, 8). Similarly, the incorporation of isovalent non-reducible elements, such as Zr^{4+} ions into ceria lattice has a beneficial effect on the structural/electronic properties of CeO_2-based catalysts, thus improving their thermal stability, oxygen storage capacity (OSC) and oxygen mobility in the solid (9). These physico-chemical properties render the metal oxidation catalysts highly active in oxidation reactions kinetically modelled via a MvK-type mechanism (9, 10). Examples of such redox mechanisms are known also in homogeneous catalysis, *i.e.* in the Wacker process, consisting typically of the conversion of ethene into acetaldehyde by oxygen in water in the presence of catalytically active Pd^{2+} and Cu^{2+} reagents (11).
Synergies in catalysis typically arise through phase-cooperation (namely, the structural relations among atoms/ions/electrons) and spillover effects. Grasselli (12) first introduced the concept of "phase-cooperation" for oxidation and ammoxidation reactions. For instance, it has been observed that both α-$Bi_2Mo_3O_{12}$ and γ-Bi_2MoO_6 phases are needed to carry out the oxidation/re-oxidation functions, through their complementary properties.
It appears that two phases (*A* and *B*) of different properties, when brought into contact with each other (*AB phase*) may lead to better catalytic performances (i.e. in terms of reaction yield) than those that can be reached by the two phases acting separately and independently from each other (10). The magnitude of the phase-cooperation can be expressed as follows:

$$\Delta Y = Y_{AB} - (W_A Y_A + W_B Y_B)$$

Where Y_{AB}, Y_A and Y_B denotes the yields of the *AB* phase, phases *A* and *B*, respectively, measured under the same operating conditions; W_A and W_B are the weight percentages of the phases *A* and *B* in the binary phase (11, 12).

On the other hand, spillover phenomenon involves the transport of active species (e.g. oxygen, hydrogen, etc.) adsorbed on one phase (donor) onto a second phase (acceptor) which does not form the active species under the same conditions (13, 14). When the catalytic sites are "irrigated" by spillover species, the solid surface significantly improves its chemical reactivity (13-15); indeed, the presence of spillover phenomena allows the solid catalysts to act more effectively (16). Similar phenomena can be observed in enzymatic catalysis by the concept of allostery (17). Accordingly, Delmon et al. (18) proposed the "remote-control" concept to explain the fact that many industrial catalysts used for the partial oxidation of hydrocarbons are multiphasic, and that specific phase compositions lead to synergistic phenomena.
In the present work, we investigate synergistic and cooperative phenomena in both homogeneous and heterogeneous catalysis via a formal classification of the catalytic systems with the combination of game theory and hyperstructure theory. Game theory is based on the idea that players are rational decision-makers (18, 19), thus here we make a transposition and we consider the chemical choice as rational. Hyperstructure theory has recently been used as a model to describe the complexity of catalysts (5, 6). Three catalytic reactions, with different numbers of products, will be used as paradigms: the degradation of azo-dye (Acid Orange 7) with vanadium/hydrogen peroxide/ascorbic acid solutions (homogeneous catalysis), the total oxidation of ethene and the carbon monoxide oxidation over Cu-Ce mixed oxide catalysts (heterogeneous catalysis).

RESULTS AND DISCUSSION

Degradation of azo-dye using vanadium/H_2O_2/ascorbic acid systems (homogeneous catalysis)

Experiments were carried out with a 10^{-3} M solution of acid orange 7 (A07), a "probe molecule" for many azo-dyes. Tests were performed at room temperature in "dark" conditions with 10 mL total volume. The component concentrations in the aqueous solution were: 20 mM ammonium metavanadate (NH_4VO_3), 80 mM hydrogen peroxide (30% H_2O_2), 80 mM ascorbic acid ($C_6H_8O_6$).
At constant time intervals, aliquots of the solution were collected. After each sampling, the UV-Vis spectrum of the solution was analyzed in the 200-600 nm range by UV-Vis spectrophotometer. The concentration of AO7 in the solution was evaluated by the intensity of the band at 484 nm, related to the hydrazone form. Degradation (%) of AO7 was calculated as $100 \cdot (C_0 - C_f)/C_0$ where C_0 and C_f are the initial and the final dye concentration (mM), respectively.

Total oxidation of ethene/co oxidation using copper-cerium mixed oxide catalysts (heterogeneous catalysis)

Preparation of the catalysts

A set of Ce-Cu mixed oxide catalysts with different Ce/Cu-contents (denoted hereafter as Cu_xCe_{1-x} where x indicates the atomic ratios of Cu/Ce+Cu) were synthesized by means of solution combustion synthesis (SCS), as described elsewhere (21). Briefly, proper amounts of $Ce(NO_3)_3$, $Cu(NO_3)_2$ and urea (in stoichiometric conditions) were dissolved in 50 mL of deionized water and stirred at room temperature for 30 min. The homogeneous solution was then placed in the oven at 600°C for 20 min. The resultant powder was washed with deionized water to remove impurities and then dried at 90°C overnight.

Catalyst characterization

The powder X-ray diffraction patterns were collected on a X'Pert Philips PW3040 diffractometer using Cu Kα radiation (2θ range = 15°- 70°; step = 0.05° 2θ; time per step = 0.2 s). The diffraction peaks were indexed according to the Powder Data File database (PDF 2000, International Centre of Diffraction Data, Pennsylvania).
Specific Surface Area (S_{BET}) and total pore volume (V_p) were measured by means of N_2 physisorption at -196°C (Micrometrics ASAP 2020) on samples previously outgassed at 200 °C for 4 h to remove water and other atmospheric contaminants. The specific surface area of the samples was calculated using the BET method.
Sample morphology was studied by a field emission scanning electron microscope (FESEM Zeiss MERLIN, Gemini-II column). The Cu/Ce-content in the samples was determined through EDS analysis (Oxford X-ACT): 5 different spots with a 10–50 nm diameter were selected in representative zones of the sample, and the average Ce/Cu-content was then calculated.

Catalytic activity tests

Catalytic activity tests were performed in a continuous reactor that is a quartz U-tube with inner diameter = 4 mm, heated by an electric furnace; temperature was measured by means of a thermocouple placed approximately in the middle of the catalytic bed.

- *Total oxidation of ethene:* The catalyst (0.1 g) was pre-treated in He (flow rate = 100 $cm^3\,min^{-1}$) for 1 h at 150°C to remove any species adsorbed on the catalyst surface. The gas flow was then switched from helium to the reactive mixture: 500 ppm ethene and 10% O_2 were fed with N_2 to the reactor with a gas hourly space velocity (GHSV) of 19100 h^{-1}. The catalytic reaction was started when the temperature was stable at 100 °C. The temperature was then raised by 5 °C/min from 100 °C up to 700 °C.
- *Carbon monoxide oxidation:* The catalyst (0.05 g) was pre-treated in He (flow rate = 50 $cm^3\,min^{-1}$) for 1 h at 50 °C. Then, 1000 ppm CO and 10% O_2 were fed with N_2 to the reactor with a GHSV of 19100 h^{-1}. The reaction was started when the temperature was stable at 50 °C. The temperature was then raised by 5 °C/min in the range from 50 to 500°C.

The gaseous mixtures were analyzed via CO/CO_2 NDIR analyzers (ABB).

RESULTS AND DISCUSSION

Definition of synergetic hyperstructures

In classical algebraic structures, the notion of group ***G*** can be interpreted with the following necessary but not sufficient condition:

$$\forall\,(a,b) \in G^2 : |ab| = 1$$

in which *a* and *b* are two elements of *G*. Moreover, in a group there is an inner operation which means that:

$$\forall (a,b) \in G^2 : |ab| = G$$

In terms of cooperation, the elements *a* and *b* may cooperate to give a product. Thus, it is possible to generalize this concept to define the "synergetic hyperstructures" with the notion of hyperoperation. According to Marty's theory, a hyperstructure is every algebraic structure in which at least one hyperoperation is defined (22). In an algebraic structure the composition of elements is still an element, while in an algebraic hyperstructure the composition of elements is a set (22, 23). In a hypergroup *H*, according to the definition of Marty (22), we have:

$$\forall (a,b) \in H^2 : \quad 1 \leq |a * b| \leq |H|$$

which is a consequence of the axioms of reproduction and associativity (5, 23-26).
In this context, we can give a more formal difference between cooperation and synergy. Specifically, the group operation is cooperation (C) but not synergy because we have only:

$$|a * b| = 1$$

On the other hand, synergy is more than cooperation, since it occurs when:

$$|a * b| > 1$$

According to the latter condition, we can define the synergetic hyperstructures (SH) as:

$$\forall (a,b) \in SH : |a * b| > 1$$

and strong synergetic hyperstructures (SSH) as:

$$\forall (a,b) \in SSH : |a * b| > 2$$

Therefore, a strong synergy has the following propriety:

$$a \cup b = \{a,b\} \subset a * b$$

These theoretical concepts may be applied to the science of catalysis, thus leading to a formal classification of the catalytic systems:

- *If there are ≥ two elements (i.e. active phases/centres) and one product can be obtained via catalysis, then it is cooperation (C).*
- *If there are ≥ two elements (i.e. active phases/centres) and two products can be obtained via catalysis, then it is a synergetic hyperstructure (SH).*
- *If there are ≥ two elements (i.e. active phases/centres) and at least three products can be obtained via catalysis, then it is a strong synergetic hyperstructure (SSH).*

Many catalytic reactions can be mentioned as characteristic examples, particularly for industrial and environmental catalysis where multicomponent catalysts are usually used. For instance, cooperation phenomena may appear in the CO oxidation over mixed oxides (e.g. ceria-doped catalysts) (27), as well as in the ammonia synthesis catalyzed by multicomponent catalysts (e.g. K-promoted iron oxides) (11, 28). Examples of synergetic hyperstructures can be observed in the total oxidation of Volatile Organic Compounds (VOC) over mixed oxide catalysts (e.g. Mn-Ce-O or Cu-Ce-O systems (10, 29)) when there are only the total oxidation products (CO_2 and H_2O). Similarly, strong synergetic hyperstructures may arise in the oxidative dehydrogenation (ODH) of light alkanes over multicomponent catalysts (e.g. V-Ti-O, V-Al-O, V-Mg-O, etc.), since several reaction products occur (e.g. alkenes, H_2, CO_x, etc.) (30, 31). It appears that the effects (e.g. catalytic benefits) of the structural relations among atoms/ions/electrons depend on the nature of catalytic system, and then a scale of magnitude should be proposed:

COOPERATION < SYNERGETIC HYPERSTRUCTURE << STRONG SYNERGETIC HYPERSTRUCTURE

This classification suggests that catalytic processes reflected by SSH and SH should exhibit better catalytic improvements, rather than reactions leading to one reaction product.

The concepts of relevance and strategic relevance
According to Hjørland and Sejer Christensen (32), something (A) is relevant to a task (T) if it increases the likelihood of accomplishing the goal (G), which is implied by T. This means that the concept of relevance is related to the task, but in strategy we need something more specific: it is necessary to codify the task as a strategic mix in order to be global and not only local. Thus, the relevance is close to the efficiency of contribution in this context. If the contribution of some elements in the strategic mix is negative (e.g. inerts, impurities, etc.) than it is not relevant. Conversely, the relevance is the positive contribution in the strategic mix, which can be passive and not active. In the last case, which means active, a strategic relevance appears in the frame of cooperation. Thus, the strategic relevance is related to the notion of cooperation. Moreover, we can make a distinction between a cooperative and a synergistic behavior: the former is a positive collaboration, whereas the latter is an efficient collaboration. The strategic relevance can be strong in the context of a synergistic behavior. Therefore, the concept of relevance, and even more of strategic relevance, is not independent of the task and it depends on the strategic mix. This means that in catalysis we have to consider the relevance as a condition and not as a result, to obtain a specific goal.

Degradation of azo-dye using vanadium (H_2O_2/ascorbic acid systems
In game theory, a game is cooperative when the players are able to form binding commitments; making a transposition we obtained the following results. The degradation of Acid Orange 7, a probe molecule for the several azo-dyes found as contaminants in both wastewater and groundwater, was examined, as in previous studies by Piumetti et al. (33, 34). The latter have shown that transition metals (i.e. V- and Fe-containing catalysts) strongly improve their oxidation activity in the presence of both H_2O_2 and ascorbic acid (HA), thus leading to effective degradation of A07 via complex redox

pathways, involving radical species (Fenton-like processes). In the present study, however, the A07 degradation was carried out using V species in homogeneous phase, with H_2O_2 and HA as oxidant/reductant agents. This catalytic system in normal form is a structure:

$G = \langle P, \mathbf{S}, \mathbf{F} \rangle$

where

$P = \{V, H_2O_2, HA\}$

is a set of players,

$\mathbf{S} = \{S_V, S_{H2O2}, S_{HA}\}$

is a 3-tuple of pure strategy sets, one for each player,

$\mathbf{F} = \{F_V, F_{H2O2}, F_{HA}\}$

is the 3-tuple of payoff functions.

Finally, we use the degradation ($= 100 \cdot (C_0 - C_f)/C_0$) as payoff function.

Figure 1 shows the Venn diagrams of $V/H_2O_2/HA$ and their initial concentrations in A07 solution. Thus, seven combinations are possible by considering the reactive components (players) in solution: V, H_2O_2 and HA (one component or player in the sense of decision theory); V/H_2O_2, V/HA and H_2O_2/HA (two components or players in the sense of game theory); $V/HA/H_2O_2$ (three components or players).
In this scenario, the catalytic reaction represents a synchronous game, since each player acts simultaneously over the reaction time (19). Moreover, it is a not-zero-sum game, since the outcome has net results greater (or lesser) than zero. The players have a finite number of pure strategies, reflected by their concentrations and play a strategic game (19, 20); moreover, they are in the Nash equilibrium (NE), since each player is making the best possible action in a cooperative-game, taking into account the actions of the other players (35). In other words, each strategy in NE is the best response to all other possible strategies in that equilibrium.

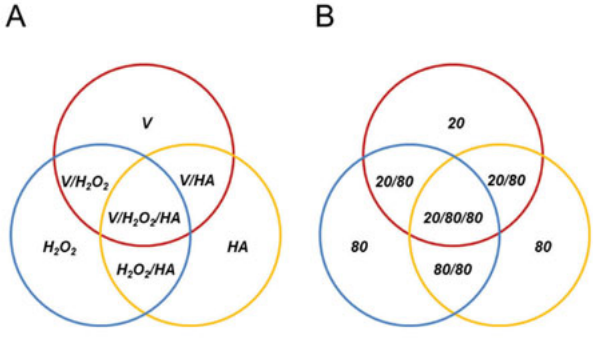

Figure 1. Venn diagrams of vanadium (V); hydrogen peroxide (H_2O_2); ascorbic acid (HA) and their initial concentration (mM) in A07 solution (Sections A and B, respectively).

As shown in Figure 2, the lowest A07 conversion values (%) as a function of time (namely 10, 20 and 30 min.) can be obtained

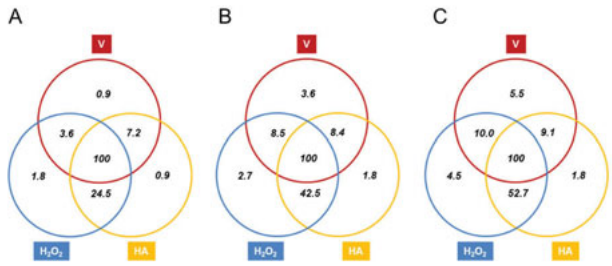

Figure 2. Venn diagrams of A07 conversion values (%) after 10, 20 and 30 min. (Section A, B and C, respectively).

for systems with just one player: the presence of either vanadium or hydrogen peroxide has a moderate effect on the degradation of A07 (around 5% degradation after 30 min.), whereas worse activity is obtained with ascorbic acid (1.8% degradation after 30 min.). Each player (V, H_2O_2 or HA) acts alone and thus its action is a pure strategy. Therefore:

$F_{HA} < F_{H2O2} < F_V$ (pure strategy)

However, with the presence of two players the A07 conversion increases slightly and the best results can be obtained with the HA/H_2O_2 system (degradation 52.7 % after 30 min.). In this case, two players (V/H_2O_2, V/HA or H_2O_2/HA) act together thus leading to a mixed strategy. Each player can choose his available pure strategies with certain probabilities, and hence there is a probability distribution to each pure strategy. J.F. Nash proved that if each player has a finite number of pure strategies, then there exists at least one equilibrium in mixed strategies (35). Thus, the payoff function of each player is maximized given the strategy of the other players, and the following order can be drawn:

$F_{V/HA} < F_{V/2O2} < F_{H2O2/HA}$ (mixed strategy)

Remarkable results may appear with vanadium in the presence of both HA and H_2O_2 (three players), thus confirming the beneficial effect of both oxidant and reductant agents in Fenton-like processes, as described elsewhere (33, 34). In this case, indeed, the presence of three active components in the systems leads to total conversion of the A07 in less than 10 min. (UV-vis spectra not reported for the sake of brevity).
The players act together with a totally mixed strategy and so it is possible to assign a strictly positive probability to every pure strategy. Therefore, the payoff function is also defined:

$F_{V/H2O2/HA}$ (totally mixed strategy).

As a result, the catalytic system is not a symmetric game, since the players cannot be changed without changing the payoff functions. The system is also in Pareto efficiency since it is not possible to improve any payoff function.
The players cooperate synergistically to decompose A07 into two reaction products, namely sulfanilic anion and 1-amino-2-naphtol (36). However, in either basic or acidic conditions, the amino group of the 1-amino-2-naphthol readily hydrolyzed to 1,2-dihydroxynaphtalene, which in turn is oxidized to o-naphthoquinone (37). As a whole, this complex process may produce several products (more than two) depending on the catalyst, pH and

reaction time. Therefore, the active components (players) cooperate synergistically in the framework of strong synergistic hyperstructures.

Total oxidation of ethene and co oxidation over copper-cerium mixed oxide catalysts

It is well-known that the oxidation of VOCs over transition metal oxides, such as CuO-CeO_2 catalysts, usually occurs via a MvK-type mechanism, and proceeds through lattice oxygens (nucleophilic attack) of the solid catalyst (37). This redox mechanism includes two steps: a hydrocarbon molecule (R-H) reacts by extracting lattice oxygen (O^{2-}) from the catalyst surface (R-H + $O^{2-} \rightarrow$ R-O^- + H^+ + 2e^-), thereby generating oxidized products and a reduced surface. Afterwards, the lattice oxygen is replenished by the reduction of gaseous oxygen (½O_2 + 2e^- → O^{2-}) (38). Then, the molecular oxygen is only required to reoxidize the catalyst surface. The MvK-type mechanism has also been proposed for the CO oxidation over ceria-based catalysts: CO reacts with surface oxygen to form CO_2 and an oxygen vacancy (step I); then, a molecule of O_2 fills in this O vacancy (step II) (27).

In this scenario, Ce-Cu mixed oxides are effective catalysts for both VOCs total oxidation and CO oxidation reactions (27, 37, 39, 40). Therefore, a set of Ce-Cu oxide catalysts with different Cu/Ce contents was prepared to study the catalytic activity for both reactions. The high redox activity of Ce-Cu mixed oxides arises by the ability to reduce and re-oxidize of both Cu^{2+}/Cu^+ and Ce^{4+}/Ce^{3+} couples, which is improved by the strong Cu-O-Ce interactions (27).

In the present study, the prepared Cu_xCe_{1-x} samples exhibit specific surface areas (SSA) and total pore volumes in the range of 3-31 m^2g^{-1} and 0.01-0.07 cm^3g^{-1}, respectively (Table 1). The highest surface area and pore volume are reached with the $Cu_{0.4}Ce_{0.6}$ catalyst, whereas further increases of Cu-contents lead to worse textural properties. Conversely, the SSA for pure CeO_2 and CuO are 21 m^2 g^{-1} and 3 m^2 g^{-1}, respectively.

Catalyst	S_{BET}[a] (m^2g^{-1})	V_p[b] (cm^3g^{-1})	r_{C2H4}[c] (mmol m^{-2} h^{-1})	r_{CO}[d] (mmol m^{-2} h^{-1})
CeO_2	21	0.05	2.1	0.00
$Cu_{0.15}Ce_{0.85}$	24	0.06	5.5	23.2
$Cu_{0.40}Ce_{0.60}$	31	0.07	8.9	40.1
$Cu_{0.60}Ce_{0.40}$	25	0.06	10.3	24.9
$Cu_{0.85}Ce_{0.15}$	16	0.02	8.1	5.2
CuO	3	0.01	4.1	0.0

Table 1. Textural properties and specific oxidation rates of the Ce-Cu mixed oxide catalysts.

[a] S_{BET} = specific surface area.
[b] V_p = total pore volume.
[c] r_{C2H4} = Specific C_2H_4 oxidation rate (at 300 °C).
[d] r_{C2H4} = Specific CO oxidation rate (at 100 °C).

As a whole, a cubic fluorite lattice structure of ceria (*Fm3m* symmetry) appears for all Cu-Ce mixed oxide catalysts. Reflections of the copper oxide (CuO) phase can be observed in the addition to those of ceria, as the increase of copper leads to the formation of bulk CuO particles. Moreover, relatively uniform agglomerates of particles (diameter of ca. 100-150 nm) appear for all the prepared catalysts (XRD diffractograms and FESEM images not reported for the sake of brevity).

The conversion of ethene to CO_2 (C_2H_4 + 3O_2 → 2CO_2 + 2H_2O) as a function of temperature over the Ce-Cu oxide catalysts is shown in Figure 3. All the catalysts display positive conversion trends for an increasing reaction temperature. However, different activity trends can be observed. The most active catalyst is the $Cu_{0.60}Ce_{0.40}$ (total conversion of ethene occurs below 450 °C), whereas higher Cu-contents reduce the catalytic performances. Conversely, the lowest conversion values are achieved for pure CeO_2 (total conversion obtained at 736°C). Indeed, Ce-Cu mixed oxide catalysts show better activities compared to either CuO or CeO_2, due to their easier reducibility and better redox properties (37, 39, 40), as revealed by H_2-TPR and XPS analysis (data not reported for the sake of brevity). On the other hand, the beneficial effect of the SSA on the overall oxidation activity may be also possible.

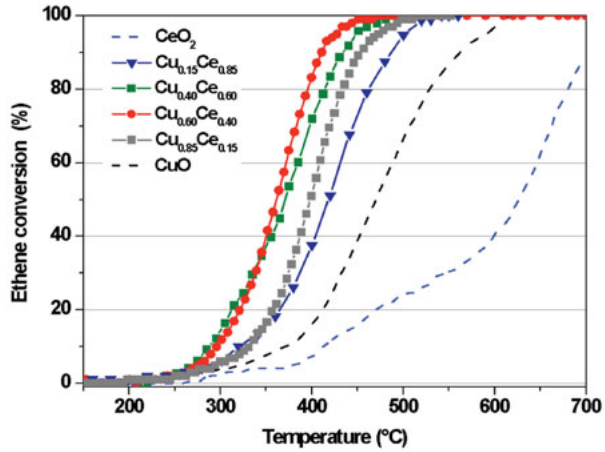

Figure 3. Conversion of ethene to CO_2 as a function of temperature over the Ce-Cu oxide catalysts.

These findings show that Ce-Cu mixed oxides (two players) cooperate synergistically to lead higher oxidation activities than those reached by either CuO or CeO_2 phase (one player). The magnitude of this synergy (payoff function) depends on the Cu/Ce ratio, which is the mixed strategy used to carry out the strategic game. The catalytic system displays the Pareto efficiency for each mixed strategy, although different payoff function values appear. Figure 4 show the temperature at which 50% ethene conversion to CO_2 (denoted as $T_{50\%}$) is attained over the Ce-Cu oxide catalysts. Since conversion values depend on GHSV, weight of catalyst and many other variable that make comparison with other systems a difficult task, it has been calculated the specific ethene oxidation rate for each catalyst under kinetic control (see Table 1). These results confirm that the co-presence of CeO_2 and CuO phases has a beneficial effect

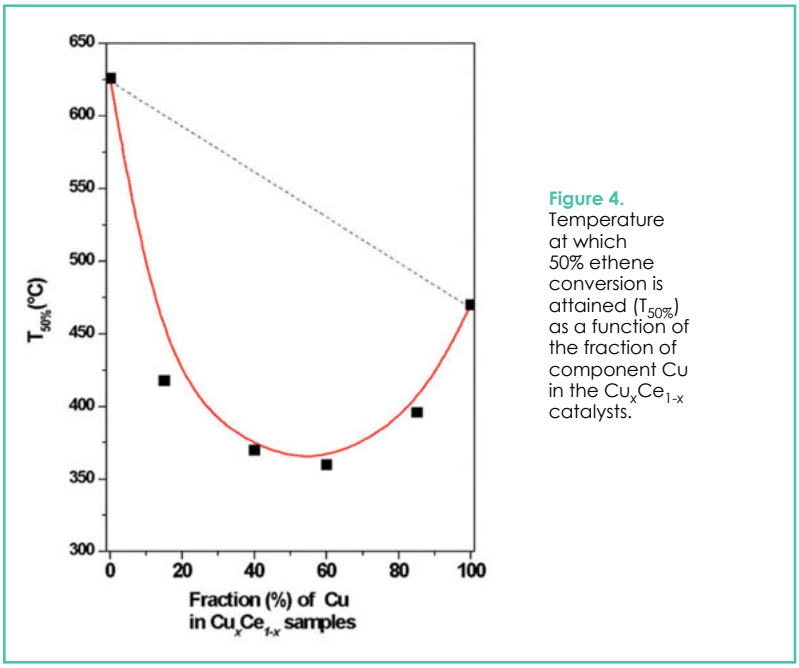

Figure 4. Temperature at which 50% ethene conversion is attained ($T_{50\%}$) as a function of the fraction of component Cu in the Cu_xCe_{1-x} catalysts.

on the structural and electronic properties of the catalysts, and the best catalytic performances can be obtained for intermediate compositions (Cu/Ce atomic ratio ~ 1.5). Since CeO_2 and CuO phases cooperate synergistically, giving rise to two oxidation products (CO_2 and H_2O), then this catalytic system is an example of synergetic hyperstructure. Likewise, the CO oxidation reaction over the same catalysts (Figure 5) shows the presence of a cooperative-game, in which the players act simultaneously to maximize the payoff function (here defined as "CO_2 production"). In the present case, however, the best mixed stategy is obtained for Cu/Ce atomic ratio ~ 0.7 ($T_{50\%}$ values and specific CO oxidation rates are reported in Figure 6 and Table 1, respectively) and this catalytic system reflects a cooperation among the players, since CO_2 is the only reaction product.

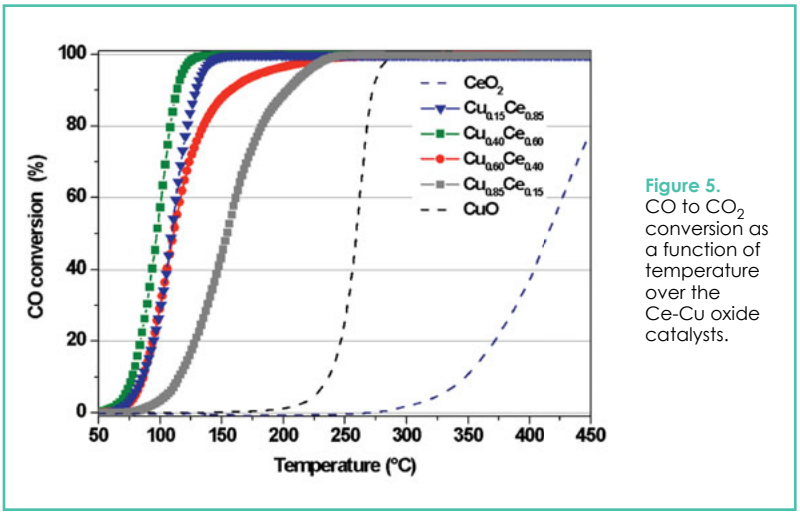

Figure 5. CO to CO_2 conversion as a function of temperature over the Ce-Cu oxide catalysts.

CONCLUSIONS

We have considered the synergistic and cooperative phenomena that may occur in catalytic reactions, introducing a formal classification of the catalytic systems, via the combination of game theory and hyperstructure theory. Three catalytic reactions have been considered:

- The degradation of Acid Orange 7 with V/H_2O_2/HA (= strong synergetic hyperstructure);

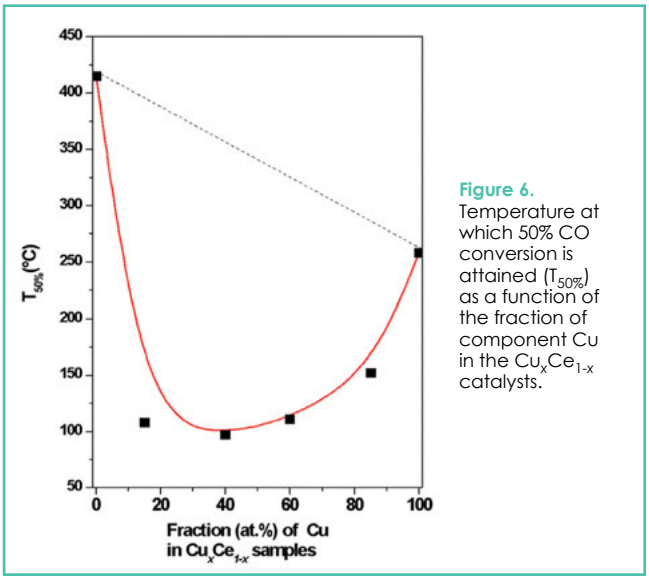

Figure 6.
Temperature at which 50% CO conversion is attained ($T_{50\%}$) as a function of the fraction of component Cu in the Cu_xCe_{1-x} catalysts.

- The total oxidation of ethene over Cu-Ce mixed oxide catalysts (= synergetic hyperstructure);
- The carbon monoxide oxidation over Cu-Ce mixed oxide catalysts (= cooperation).

According to the game theory, these reactions are characteristic examples of not-zero sum, asymmetrical and synchronous cooperative-games. The players (i.e. active phases/centres) exhibit a finite number of pure strategies, reflected by their concentrations, and play a strategic game. Moreover, there is the Nash equilibrium and even Pareto equilibrium in the synergistic case. Since the effects of the structural relations among players depend on the system, a scale of magnitude (in terms of catalytic benefits) has been proposed: cooperation < synergetic hyperstructure << strong synergetic hyperstructure. This means that multicomponent systems may operate through sophisticated self-organizing phenomena taking place on the catalyst surface, in which both structural and chemical complexity play a role. This suggests that catalytic processes reflected by SSH and SH should exhibit better catalytic improvements over multicomponent catalysts, rather than reactions leading to one reaction product. However, experimental studies are still necessary to provide evidence of these concepts and reveal the benefits for applied catalysis.

REFERENCES

1. R.A. Van Santen, M. Neurock M., Molecular Heterogeneous Catalysis, Wiley-VCH, Weinheim (2006) pp. 61-62.
2. O. Deutshmann, H. Knözinger, K. Kochloefl, T. Turek, Heterogeneous Catalysis and Solid Catalysts, 7th ed., Weinheim, Wiley-VCH, 2009.
3. J.C. Vedrine, Appl. Catal. A 474, pp. 40-50 (2014).
4. M. Piumetti, N. Lygeros, Chem. Today 31, pp. 48–52 (2013).
5. M. Piumetti, N. Lygeros, Hadronic J. 36, pp. 177-195 (2013)
6. M. Piumetti, N. Lygeros, Chem. Today 33, pp. 48-52 (2015)
7. G. Carson, J.C. Coudurier, A. Védrine, F. Laarif, Theobald, J. Chem. Soc. Faraday Trans. I 79, pp. 1921-1929 (1983).
8. J.M.M. Millet, H. Ponceblanc, G. Coudurier, J.M. Herrmann, J.C. Védrine, J. Catal.142, pp. 381-391 (1993).
9. M. Piumetti, F.S. Freyria, B. Bonelli, Chem. Today 31, pp. 55–58 (2013).
10. A. Trovarelli, P. Fornasiero, Catalysis by Ceria and Related Materials (2nd ed.), Imperial College Press, London (2013) pp. 565-621.
11. G. Ertl, H. Knözinger, F. Schüth, J. Weitkamp, Handbook of Heterogeneous Catalysis, 2nd ed., Weinheim, Wiley-VCH (2008) pp. 3684-3700.
12. R. K. Grasselli, Top. Catal. 15, 93-101 (2001)
13. M. Boudart, J. Mol. Catal. A 138, pp. 319-321 (1999).
14. W. Curtis Conner, J.L. Falcone, Chem Rev. 95, pp. 759-788 (1995)
15. E.M. Gaigneaux, H.M. Abdel Dayem, E.Godard, P. Ruiz, Appl. Catal. A 2002, pp. 265-283 (2000).
16. G.M. Pajonk, Appl. Catal. A 202, pp. 157-169 (2002)
17. B. Delmon, Heterog. Chem. Rev. 1, pp. 219-230 (1994).
18. L.-T. Weng, B. Delmon, Appl. Catal. A 81, pp. 141-213 (1992).
19. D. Fudenberg, J. Tirole, Game Theory, MIT Press (1991)
20. J. von Neumann, O. Morgenstern, Theory of games and Economic Behavior, John Wiley Science Ed. (1964).
21. D. Delimaris, T. Ioannides, Appl. Catal. B 89, pp. 295-302 (2009).
22. F. Marty, Sur une généralisation de la notion de groupe, 8th Congress Math. Stockholm, pp. 45-49 (1934).
23. T. Vougiouklis, New Frontiers in Hyperstructures, Hadronic Press, Palm Harbor, 48 (1996).
24. T. Vougiouklis, Hyperstructures and their representations, Hadronic Press Inc., Florida (1994).
25. N. Lygeros, T. Vougiouklis, Ratio Math., 25, pp. 59-66 (2013).
26. B. Davvaz, R.B. Santilli, T. Vougiouklis, Proc. 3th Int. Conf. Treat. Irrev. Proc.. (Kathmandu University, Nepal), 1-12 (2011).
27. S. Royer, D. Duprez, ChemCatChem 3 pp. 24-65 (2011).
28. G. Ertl, Reactions at Solid Surfaces, Ed. Wiley-VCH, Hoboken, 2009.
29. D. Duprez, F. Cavani, Handbook of Advanced Methods and Processes in Oxidation Catalysis, Imperial College Press, 2014.
30. F. Cavani, F. Trifirò, Catal. Today 24, pp. 307-313 (1995)
31. F. Cavani, N. Ballarini, A. Cericola, Catal. Today 127, pp. 113–131 (2007).
32. B. Hjørland, F. Sejer Christensen, JASIST 53(11), pp. 960-965 (2002)
33. M. Piumetti, F. S. Freyria, M. Armandi, F. Geobaldo, E. Garrone, B. Bonelli, Catal. Today 227, pp. 71-79 (2014)
34. M. Piumetti, F. S. Freyria, M. Armandi, G. Saracco, E. Garrone, B. Bonelli, Chem. Today 33(3), pp. 40-45 (2015).
35. J. Cao, L. Wei, Q. Huang, L. Wang, S. Han, Chemosphere 38, pp. 565-571 (1999)
36. F.S. Freyria, B. Bonelli, R. Sethi, M. Armandi, E. Belluso, E. Garrone, J. Phys. Chem. C 115, pp. 24143-24152 (2011)
37. V. Balcaen, H. Poelman, D. Poelman, G.B. Marin, J. Catal. 283, pp. 75-88 (2011).
38. M. Piumetti, D. Fino, N. Russo, Appl. Catal. B 163, pp. 277-287 (2015).
39. P.M. Heynderickx, J.W. Thybaut, H. Poelman, D. Poelman, G.B. Marin, J. Catal. 272, pp. 109-120 (2010).
40. U. Menon, V.V. Galvita, G.B. Marin, J. Catal. 283, pp. 1-9 (2011)